Vol. 4, 833–840, April 1998

Advances in Brief

Adenovirus-mediated *p53* Gene Therapy and Paclitaxel Have Synergistic Efficacy in Models of Human Head and Neck, Ovarian, Prostate, and Breast Cancer

Loretta L. Nielsen,[1] Philip Lipari, Janet Dell, Maya Gurnani, and Gerald Hajian

Tumor Biology [L. L. N., P. L., J. D., M. G.] and Biostatistics [G. H.], Schering-Plough Research Institute, Kenilworth, New Jersey 07033-0539

Abstract

Synergy (or antagonism) between two chemical agents is an *in vitro* empirical phenomenon, in which the observed effect of the combination is more (or less) than what would be predicted from the effects of each agent working alone. Although mathematical synergy is not directly provable in the clinical setting, it does predict a favorable outcome when the two therapeutics are combined *in vivo* and strongly suggests the presence of *in vivo* synergy. In contrast, overt antagonism warns of future problems. Sophisticated three-dimensional statistical modeling was used to evaluate the presence of synergistic, additive, or antagonistic efficacy between adenovirus (Ad)-mediated *p53* gene therapy (p53 Ad) and paclitaxel (Taxol) in a panel of human tumor cell lines. Cells were either pretreated with paclitaxel 24 h before p53 Ad or treated with both agents simultaneously. Cell proliferation was measured 3 days later. Paclitaxel had synergistic or additive efficacy with *p53* gene therapy. In no case was the interaction antagonistic. Cell cycle analysis demonstrated that p53 Ad arrested cells in G_0/G_1 prior to apoptotic cell death, whereas paclitaxel arrested cells in G_2-M prior to apoptotic cell death. When combined, the relative concentration of each agent determined the dominant cellular response. These results are consistent with the previously reported cell cycle effects of p53 or paclitaxel, respectively; however, these data fail to explain the observed drug synergy. We found that low concentrations of paclitaxel (1–14 nM) increased the number of cells transduced by recombinant Ad 3–35% in a dose-dependent manner, which is one possible mechanism for the observed synergy. Of particular note, the concentrations of paclitaxel responsible for increased Ad transduction were lower than the concentrations required for microtubule condensation. The efficacy of combination therapy was also evaluated *in vivo*. In the $p53^{mut}$ SK-OV-3 xenograft model of ovarian cancer, a dosing schedule of p53 Ad that, by itself, had a relatively minimal effect on tumor burden (16%) caused a much greater decrease in tumor burden (55%) when combined with paclitaxel. Greater combined efficacy was also observed in the $p53^{mut}$ DU-145 prostate, $p53^{mut}$ MDA-MB-468 breast, and $p53^{mut}$ MDA-MB-231 breast cancer xenograft models *in vivo*. In summary, p53 Ad for cancer shows enhanced efficacy when combined with paclitaxel. This combination is recommended for clinical cancer trials.

Introduction

p53 is a DNA-binding protein that acts as a transcription factor to control the expression of proteins involved in the cell cycle (1, 2). In response to DNA damage, p53 protein accumulates in the cell nucleus, causing cells to undergo cell cycle arrest and DNA repair or apoptosis (programmed cell death; Ref. 3). Functional inactivation of p53 can occur by several mechanisms, including direct genetic mutation, binding to viral oncoproteins or cellular factors (*e.g.*, mdm2), or alteration of the subcellular localization of the protein (1, 2). Although p53 is not essential for normal development, p53 "knockout" mice are susceptible to tumors early in life (4). Mutations in p53 have been reported in a majority of clinical cancers, and it has been estimated that p53 function is altered in half of all human malignancies (1, 2). Of particular significance, alterations in p53 are linked to poor prognosis, disease progression, and decreased sensitivity to chemotherapeutic agents. Introduction of wild-type p53 into tumors with nonfunctional p53 offers a novel strategy for treating cancer, by inducing apoptotic death in neoplastic cells (5).

Paclitaxel (Taxol) inhibits cell replication by enhancing polymerization of tubulin monomers into stabilized microtubule bundles that are unable to reorganize into the proper structures for mitosis (6, 7). This results in cell cycle blockage in mitosis and subsequent activation of an apoptotic pathway, which may be p53 independent (8, 9). The rationale for combining *p53* gene therapy with paclitaxel in the clinical setting are as follows: (*a*) combinations of agents with different toxicological profiles can result in increased efficacy without increased overall toxicity to the host; (*b*) combinations of agents may thwart the development of resistance to the single agents; (*c*) combinations of agents may offer a solution to the problem of heterogeneous tumor cell populations with different drug sensitivity profiles; and (*d*) combinations of agents can allow the physician to take advantage of possible synergies between drugs, resulting in increased anticancer efficacy in patients. Synergy (or antagonism) between two chemical agents is an *in vitro* empirical phenomenon, in which the observed effect of the combination is more (or less) than what would be predicted from the effects of each agent working alone (10). Although *in vitro* synergy is not directly provable in the clinic, it does predict a favorable out-

Received 12/2/97; revised 1/13/98; accepted 1/13/98.
The costs of publication of this article were defrayed in part by the payment of page charges. This article must therefore be hereby marked *advertisement* in accordance with 18 U.S.C. Section 1734 solely to indicate this fact.

[1] To whom requests for reprints should be addressed, at K15-4945, Schering-Plough Research Institute, 2015 Galloping Hill Road, Kenilworth, NJ 07033-0539. Phone: (908) 298-7335; Fax: (908) 298-7115.

come when the two therapeutics are combined. In contrast, overt antagonism warns of future problems.

p53 Ad[2] (ACN53) is a novel gene therapy for cancer (11). ACN53 consists of a replication-deficient, type 5 Ad vector expressing human *p53* tumor suppressor gene under the control of the cytomegalovirus promoter. p53 Ad has therapeutic efficacy against a wide range of human tumor types with altered p53 both *in vitro* and *in vivo* (5, 11–13). Here, we examined the efficacy of p53 Ad in combination with paclitaxel against a panel of human tumor cell lines *in vitro* and *in vivo*. Greater combined efficacy was observed in all cases. In addition, we provide evidence that paclitaxel increases the transduction of tumor cells by recombinant Ad at paclitaxel concentrations that cause minimal tumor cell death.

Materials and Methods

Cell Lines and Ad Infections in Vitro

All cell lines were obtained from American Type Culture Collection (Rockville, MD). SCC-9, SCC-15, and SCC-25 head and neck tumor cells ($p53^{null}$) were cultured in a 1:1 mixture of DMEM and Ham's F-12 (Life Technologies, Inc., Grand Island, NY) with 10% FCS (Hyclone, Logan, UT), 0.4 μg/ml hydrocortisone (Sigma Chemical Co., St. Louis, MO), and 1% nonessential amino acids (Life Technologies, Inc.) at 37°C and 5% CO_2. SK-OV-3 human ovarian tumor cells ($p53^{null}$) and DU-145 human prostate tumor cells ($p53^{mut}$) were cultured in Eagle's MEM plus 10% FCS at 37°C and 5% CO_2. OVCAR-3 ovarian tumor cells ($p53^{mut}$) were cultured in RPMI 1640 (Life Technologies, Inc.), 10 μg/ml bovine insulin (Sigma), and 20% FCS (Hyclone) at 37°C and 5% CO_2. MDA-MB-231 human mammary tumor cells ($p53^{mut}$) were cultured in DMEM (Life Technologies, Inc.) with 10% FCS (Hyclone, Logan, UT) at 37°C and 5% CO_2. MDA-MB-468 human mammary tumor cells ($p53^{mut}$) were cultured in Leibovitz's L-15 medium (Life Technologies, Inc.) containing 10% FCS (Hyclone) at 37°C without CO_2.

MDA-MB-231 mammary tumor cells carry an Arg-to-Lys mutation in codon 280 of the *p53* gene and express mutant p53 (14). DU-145 prostate tumor cells carry two mutations on different chromosomes, a Pro-to-Leu mutation in codon 223 and a Val-to-Phe mutation in codon 274 (15). They express mutant p53. SK-OV-3 ovarian tumor cells are p53 null (16). OVCAR-3 carry an Arg-to-Gln mutation in codon 248 and express mutant p53 (16). SCC-9 cells have a deletion between codons 274 and 285, resulting in a frameshift mutation (17). No immunoreactive p53 protein is detectable in SCC-9 nuclei (17–19). SCC-15 cells have an insertion of 5 bp between codons 224 and 225. They produce low levels of p53 mRNA but no detectable p53 protein (19). SCC-25 cells have loss of heterozygosity at chromosome 17 and a 2-bp deletion in codon 209 on the remaining allele (18). p53 mRNA is not detectable in SCC-25 cells, and no immunoreactive p53 protein is observed in their nuclei (18).

Construction and propagation of the human wild-type p53 and *Escherichia coli* β-gal Ads have been described previously (11). The concentration of infectious viral particles was determined by measuring the concentration of viral hexon protein-positive 293 cells after a 48-h infection period (20). Ads were administered in phosphate buffer [20 mM NaH_2PO_4 (pH 8.0), 150 mM NaCl, 2 mM $MgCl_2$, and 2% sucrose]. For *in vitro* studies with p53 Ad, cells were plated at a density of 1.5×10^4 cells/well on a 96-well plate and cultured for 4 h at 37°C and 5% CO_2. Paclitaxel, p53 Ad, or the appropriate vehicle was added to each well, and cell culture was continued overnight. Then p53 Ad, paclitaxel, or the appropriate vehicle was added to each well. Cell culture was continued for an additional 2 days. Cell proliferation was measured using the MTT assay (21). Briefly, 25 μl of 5 mg/ml MTT vital dye were added to each well and allowed to incubate for 3–4 h at 37°C and 5% CO_2. Then, 100 μl of 10% SDS detergent were added to each well, and the incubation was continued overnight. Fluorescence in each well was quantitated using a Molecular Devices microtiter plate reader.

Statistical Analysis

Data from drug interaction studies were analyzed using nonparametric response surface methodology (22). The three-dimensional (*X*, *Y*, and *Z*) response surface consisted of the paclitaxel dose, the p53 Ad dose, and the response (cell proliferation expressed as a percentage), respectively. The three-dimensional response surface data were fitted with a bivariate spline (23) using PROC G3GRID in the statistical package SAS (24). Isobolograms were computed from the fitted response surface (25) using PROC GCONTOUR in SAS (24). Statistical evaluation of the isobologram used the interaction index (26) to determine synergism, antagonism, and additivity (27). PROC TRANSREG in SAS (28) was used to compute the *Ps* for the interaction term in the bivariate spline. Also, the fitted values were compared with the observed values to determine the goodness of fit.

Cell Cycle Analysis by FACS

MDA-MB-231 cells were used in experiments designed to study cell cycle kinetics after treatment with p53 Ad, paclitaxel, or both. Cells were incubated with 0, 15, 30, 60, or 100 m.o.i. (CIU/cell) p53 Ad in combination with 0, 10, 15, 30, 45, or 60 ng/ml paclitaxel under normal culture conditions for 24 or 48 h. At the end of the incubation period, cells were washed with PBS (2×) and resuspended in ice-cold 70% methanol in PBS for a minimum of 15 min. The cells were washed with PBS (2×) and resuspended in 0.5 ml of 2% fetal bovine serum in PBS with 5 μg/ml RNase A and incubated for 15–30 min at 37°C. The cells were transferred to test tubes containing 0.5 ml of 100 μg/ml propidium iodide in PBS. Ten thousand cells were counted in each sample, and the number of samples per treatment ranged from 1 to 15 for each time period. The number of cells in each phase of the cell cycle was quantitated using a FACS Vantage cell sorter (Becton Dickinson) and analyzed using Modfit% software (Verity Software).

[2] The abbreviations used are: p53 Ad, adenovirus-mediated *p53* gene therapy; Ad, adenovirus; β-gal, β-galactosidase; CIU, cellular infectious unit(s); MTT, 3-(4,5-dimethylthiazol-2-yl)-2,5-diphenyltetrazolium bromide; FACS, fluorescence-activated cell sorting; m.o.i., multiplicity of infection; scid, severe combined immunodeficiency; 5-FU, 5-fluorouracil.

Table 1 Statistical analysis of the drug interactions between p53 Ad and paclitaxel *in vitro*

Cell line	p53 protein	Cell type	Greater combined efficacy?	
			Paclitaxel first	Simultaneous
SK-OV-3	Null	Ovarian	Synergy ($P \leq 0.0002$)	Synergy ($P \leq 0.0001$)
SCC-9	Null	Head and neck	Synergy ($P \leq 0.0040$)	Synergy ($P \leq 0.0001$)
SCC-15	Null	Head and neck	Synergy ($P \leq 0.0001$)	Synergy ($P \leq 0.0001$)
SCC-25	Null	Head and neck	Synergy ($P \leq 0.0002$)	Additive ($P = 0.5835$)
OVCAR-3	Mutated	Ovarian	Additive ($P = 0.0710$)	Synergy ($P \leq 0.0001$)
DU-145	Mutated	Prostate	Additive ($P = 0.0842$)	Synergy ($P \leq 0.0001$)
MDA-MB-231	Mutated	Mammary	Synergy ($P \leq 0.0001$)	Synergy ($P \leq 0.0001$)
MDA-MB-468	Mutated	Mammary	Synergy ($P \leq 0.0001$)	ND[a]

[a] ND, not determined (unable to do analysis because cells were too easily killed by p53 Ad alone during the 3-day incubation).

Ad Transduction Studies

Cells ($1–1.5 \times 10^5$) were plated into each well of a 12-well cell culture plate on day 0. Paclitaxel and 2–5 m.o.i. β-gal Ad was added to the cell culture medium in each well. Paclitaxel concentrations were chosen from the dose-response curves for each cell line and ranged from 0 to 12 ng/ml (0–14 nM). Those concentrations had synergistic or additive efficacy with p53 Ad but minimal cell killing for treatment with paclitaxel alone. On day 3, cells were fixed in 0.2% glutaraldehyde and washed in PBS. To assay for β-gal activity, the cells were then incubated in 1 ml of assay buffer [1.3 mM $MgCl_2$, 15 mM NaCl, 44 mM HEPES buffer (pH 7.4), 3 mM potassium ferricyanide, 3 mM potassium ferrocyanide, and 1 mg/ml 5-bromo-4-chloro-3-indolyl-β-D-galactopyranoside in *N,N*-dimethylformamide (10% final concentration)] for 5–6 h. The number of individual cells scoring positive or negative for β-gal activity was counted in each microscope field. The results from three microscope fields were averaged for each well, and three wells per treatment group were used for the analysis. 5-Bromo-4-chloro-3-indolyl-β-D-galactopyranoside was purchased from Boehringer Mannheim (Indianapolis, IN). All other chemicals were purchased from Sigma.

Microtubule Immunofluorescent Microscopy

Cells were incubated overnight on 15-mm² coverslips placed in 12-well tissue culture plates at 37°C and 5% CO_2. Next, paclitaxel was added to the medium in varying concentrations, and the cells were incubated for another 24 h. The cells were then fixed in 3.7% formaldehyde in PBS for 10 min, washed with PBS, incubated with 2% Triton X-100 (which was added for 5 min), washed twice with PBS for 5 min per wash, and incubated with anti-β-tubulin monoclonal antibody (Sigma T-4026) for 1 h at 37°C. Cells were rinsed twice in PBS for 5 min per wash and then incubated with fluorescein-conjugated antimouse IgG antibody (Cappel 55493) for 1 h at 37°C. After washing twice in distilled water, coverslips were applied cell side down into fluorescent mounting medium (Dako S3023) on microscope slides.

Ad Treatment in Vivo

C.B.17/ICR-scid mice were purchased from Taconic Farms (Germantown, NY) or Charles River Laboratories (Wilmington, MA). All mice were maintained in a VAF barrier facility, and all animal procedures were performed in accordance with the rules set forth in the NIH Guide for the Care and Use of Laboratory Animals. Paclitaxel was purchased from CalBiochem (San Diego, CA) or from Sigma. For *in vivo* experiments, paclitaxel was dissolved in 1:1 absolute ethanol and Cremophor EL (Sigma) and then diluted 1:10 into 0.9% saline immediately prior to i.p. injection.

SK-OV-3 Ovarian Tumor Model. In experiment 1, female scid mice were injected with 1×10^7 SK-OV-3 cells i.p. on day 0. Mice were dosed with drugs i.p. on days 7, 12, 15, and 19 in a total injection volume of 0.2 ml (drugs were mixed immediately prior to injection). The p53 Ad dose was 2.5×10^8 CIU/mouse/day (5.2×10^9 viral particles). The paclitaxel dose was 10 mg/kg/day. Tumors were harvested and weighed on day 21. There were 9 or 10 mice per group. In experiment 2, female scid mice were injected with 1×10^6 SK-OV-3 cells i.p. on day 0. Mice were dosed with drugs i.p. on days 6, 8, 10, 13, 15, and 17 in a total injection volume of 0.2 ml. The p53 Ad dose was 5×10^8 CIU/mouse/day (1×10^{10} viral particles). The paclitaxel dose was 5 mg/kg/day. Tumors were harvested and weighed on day 27. There were 9 or 10 mice per group. Graphs show mean tumor burden (in g) ± SE.

DU-145 Prostate Tumor Model. Male scid mice were injected with 2.5×10^6 DU-145 cells i.p. on day 0. Mice were dosed i.p. on days 7, 9, 11, 14, 16, and 18. Mice received a 0.2-ml total volume (0.1 ml of paclitaxel vehicle or paclitaxel plus 0.1 ml of Ad buffer or p53 Ad). The p53 Ad dose was 5×10^8 CIU/mouse/day (1.03×10^{10} viral particles). The paclitaxel dose was 1 mg/kg/day. Tumors were harvested and weighed on day 37. There were 10 mice per group. Graphs show mean tumor burden (in g) ± SE.

MDA-MB-468 Mammary Tumor Model. Each female scid mouse was injected with 1×10^7 MDA-MB-468 cells into a mammary fat pad 11 days before the start of dosing on day 0. The p53 Ad dose was 5×10^8 CIU/mouse/day (1.03×10^{10} viral particles) given on days 0–4 and 7–10. All virus injections were peri-/intratumoral. The paclitaxel dose was 10 mg/kg/day i.p., given concurrently with p53 Ad or Ad buffer. There were 10 mice per group. Tumor growth curves show mean tumor volume ± SE. Tumor volumes for different treatment groups on each day were compared by Student's *t* test using Statview II software (Abacus Concepts, Berkeley, CA).

MDA-MB-231 Mammary Tumor Model. Female scid mice were injected with 5×10^6 MDA-MB-231 cells into the mammary fat pad 11 days before the start of dosing on day 0. The paclitaxel dose was 10 mg/kg/day given i.p. The p53 Ad dose was 5×10^8 CIU/mouse/day (1.03×10^{10} viral particles), intra-/

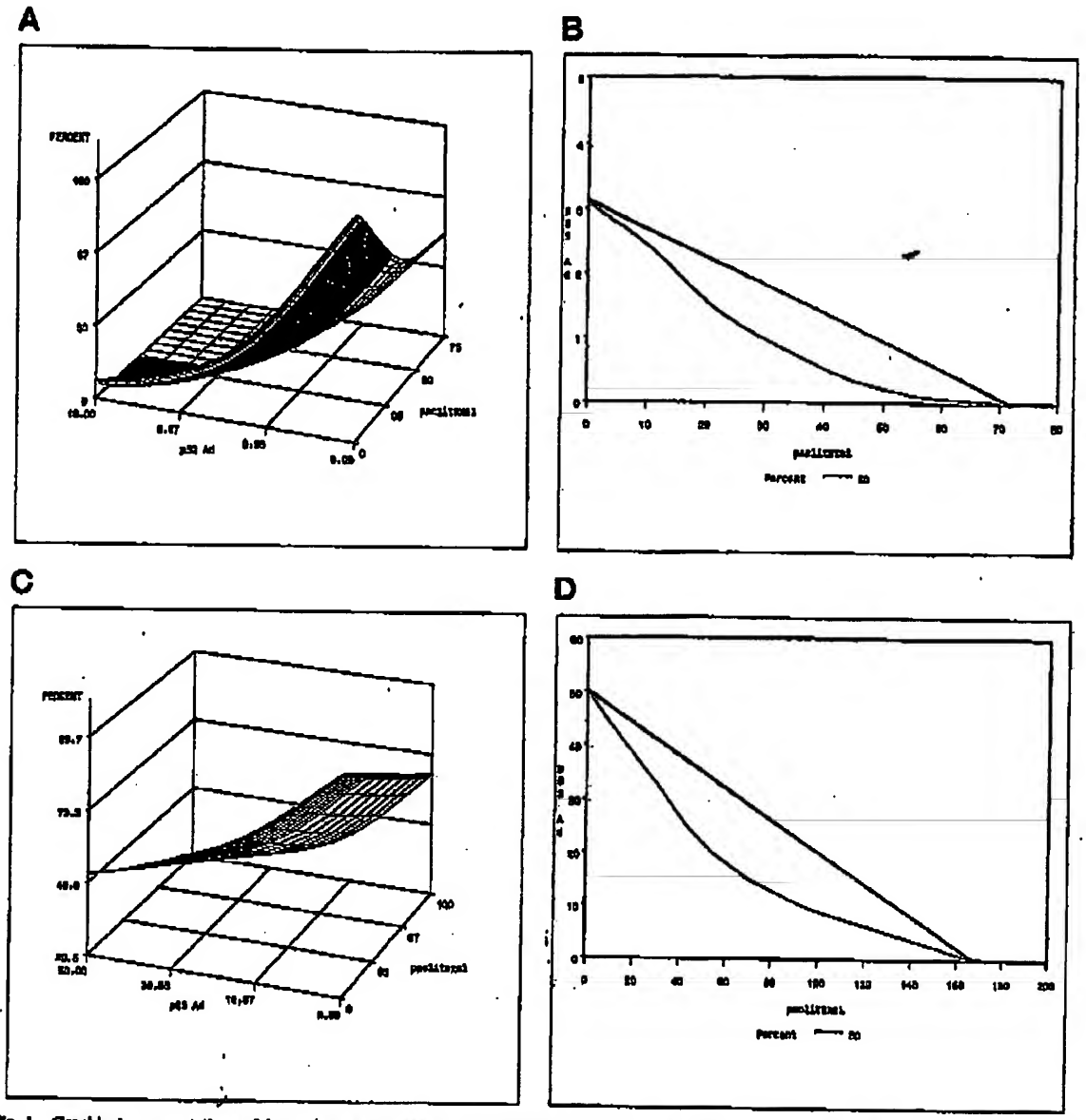

Fig. 1 Graphical representations of the statistical analyses for drug interaction in tumor cells. Cells were treated with paclitaxel 24 h before exposure to p53 Ad. *A* and *C*, dose-response surface model for various concentrations of p53 Ad and paclitaxel. *B* and *D*, isobologram with the curved dose response below and to the left of the isobole (additivity) line, demonstrating the presence of drug synergy *in vitro*. ED_{50} values were used to generate the isobole graphs. *A* and *B*, MDA-MB-468 mammary tumor cells; *C* and *D*, SCC-15 head and neck tumor cells. *Y* axis, p53 Ad (CIU/cell); *X* axis, paclitaxel (ng/ml); *Percent*, percentage cell proliferation as measured by an MTT assay.

peritumoral, on days 0–4 and 8–11. There were 10 mice per group. Tumor growth curves show mean tumor volume ± SE.

Results

Drug Interactions *in Vitro*. A summary of results from the statistical analyses of drug interactions in tumor cells is given in Table 1. Cells were treated with paclitaxel 24 h before exposure to p53 Ad or with both drugs simultaneously. Multiple dose-response curves quantitating the antiproliferative properties of different combinations of p53 Ad and paclitaxel were modeled in three dimensions. The fitted models were statistically compared with the observed values to confirm the good-

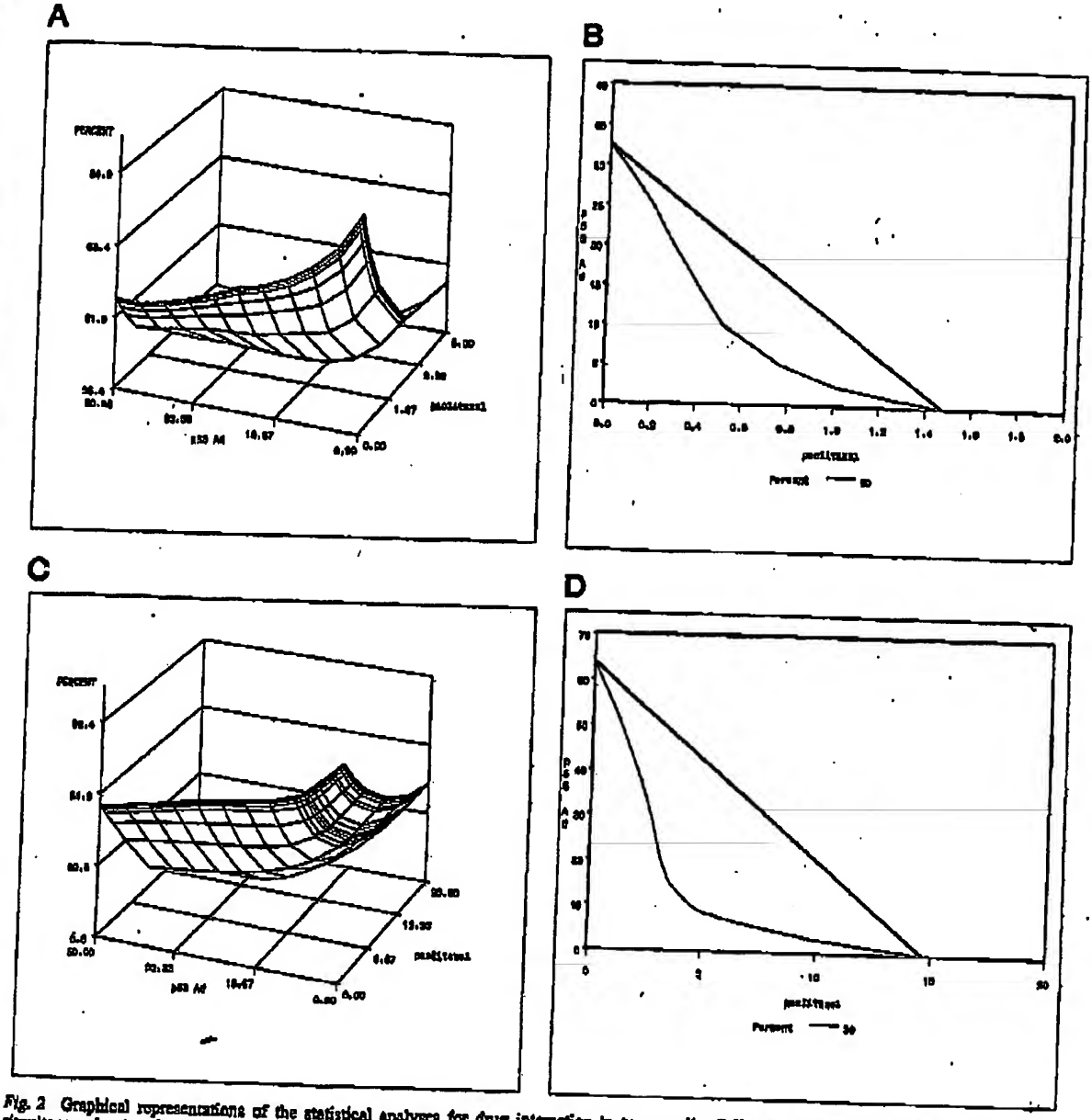

Fig. 2 Graphical representations of the statistical analyses for drug interaction in tumor cells. Cells were treated with p53 Ad and paclitaxel simultaneously. *A* and *C*, dose-response surface model for various concentrations of p53 Ad and paclitaxel. *B* and *D*, isobologram with the curved dose response below and to the left of the isobole (additivity) line, demonstrating the presence of drug synergy *in vitro*. ED_{50} (*B*) or ED_{90} (*D*) values were used to generate the isobole graphs. *A* and *B*, SK-OV-3 ovarian tumor cells; *C* and *D*, SCC-15 head and neck tumor cells. *Y* axis, p53 Ad (CIU/cell); *X* axis, paclitaxel (ng/ml); *Percent*, percentage cell proliferation as measured by an MTT assay.

ness of fit. Then Isobolograms were generated from the models to determine the presence of synergy, additivity, or antagonism between p53 Ad and paclitaxel. Synergistic antiproliferative activity was observed in all eight tumor cell lines from four distinct tissues (ovary, head and neck, prostate, and breast).

Figs. 1 and 2 show graphical representations of the statistical modeling used to analyze the drug interactions between p53 Ad and paclitaxel. Analysis of the data by an alternate model (thin plate spline) confirmed the "robustness" of our results (Ref. 29; data not shown).

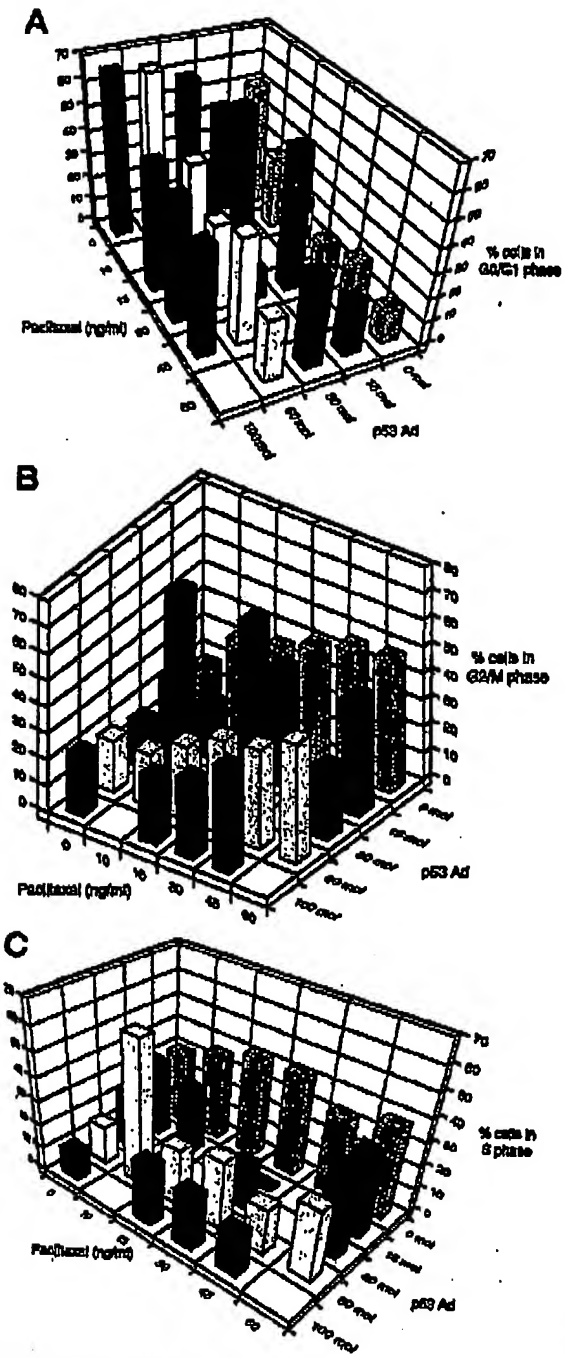

Fig. 3 Cell cycle effects of p53 Ad and paclitaxel on MDA-MB-231 cells after an incubation period of 24 h. Fractions of cells in G_0/G_1 phase (*A*); G_2-M phase (*B*); and S phase (*C*).

Cell Cycle Analysis. MDA-MB-231 tumor cells were exposed to various concentrations of p53 Ad and paclitaxel and then were assayed by FACS after 24- or 48-h incubation periods. Fig. 3 shows a graphical summary of the proportion of MDA-MB-231 cells in each phase of the cell cycle under different treatment conditions. The data at both time periods were consistent. Increasing concentrations of p53 Ad shifted the number of cells in G_0/G_1 from 51% in untreated cells up to 67% at 100 m.o.i. By contrast, paclitaxel sharply decreased the G_0/G_1 fraction to as low as 13%. p53 Ad had little effect on G_2-M; however, paclitaxel increased G_2-M from 19% in untreated cells to as high as 57%. The effects on the fraction of cells in S phase were less consistent, but in general, p53 Ad decreased the S-phase fraction, whereas paclitaxel increased it. When the two drugs were combined, the relative concentration of each drug determined the overall cell cycle response of the population. Both drugs stimulated apoptotic cell death, as indicated by an increase in the sub-G_1 peak with increasing incubation times (data not shown).

Paclitaxel Effect on Ad Transduction Rates. The ability of paclitaxel to affect the rate of cell transduction by E1-deleted Ad was examined in a panel of tumor cells. Paclitaxel concentrations were chosen based on the dose-response curves for each cell line, such that the drug concentrations had shown greater combined efficacy with p53 Ad but minimal cell killing when cells were treated with paclitaxel alone. Paclitaxel increased the number of live tumor cells transduced by β-gal Ad 3–35% in a dose-dependent manner (Table 2). As shown in Fig. 4, paclitaxel increased the percentage of cells transduced by β-gal Ad, independent of its antiproliferative efficacy.

The effect of the paclitaxel on microtubule architecture was tested in two $p53^{null}$ and three $p53^{mut}$ cell lines (SK-OV-3, SCC-15, DU-145, MDA-MB-468, and MDA-MB-231). As expected, 43 μg/ml (50 μM) paclitaxel caused extensive microtubule condensation (Fig. 5). In contrast, the concentrations of paclitaxel that increased Ad transduction rates 3–35% had minimal effect on microtubule architecture, with increased branching being the only notable effect.

Efficacy in the SK-OV-3 Ovarian Tumor Model *in Vivo*. Established SK-OV-3 tumors were treated with i.p. doses of vehicles, p53 Ad, paclitaxel, or both. In experiment 1, mice were given four doses of 2.5×10^8 CIU p53 Ad (5.2×10^9 viral particles) over a period of 3 weeks for a total virus dose of 1×10^9 CIU (2.1×10^{10} viral particles). The paclitaxel dose was 10 mg/kg/day. Tumors were harvested and weighed on day 21. The results are shown in Fig. 6. Final tumor burden in mice treated only with drug vehicles was 1.69 ± 0.05 g ($n = 9$). Treatment with p53 Ad reduced tumor burden 16% to 1.41 ± 0.06 g ($n = 10$). Treatment with paclitaxel reduced tumor burden 59% to 0.69 ± 0.04 g ($n = 10$). When both drugs were combined, there was a further 55% reduction in tumor burden over paclitaxel alone to 0.31 ± 0.03 g ($n = 10$; $P \leq 0.001$). Mice treated with vehicles or p53 Ad alone had bloody ascites and enlarged spleens. These symptoms were absent in the mice treated with paclitaxel alone or paclitaxel with p53 Ad. All livers were grossly normal.

In experiment 2, mice were given six i.p. doses of 5×10^8 CIU p53 Ad (1×10^{10} viral particles) over a period of 2 weeks for a total virus dose of 3×10^9 CIU (6.2×10^{10} viral particles). The i.p. paclitaxel dose was 5 mg/kg/day. Tumors were harvested and

Table 2 Effect of paclitaxel on Ad transduction of tumor cells *in vitro*

Cell line	Paclitaxel (ng/ml)	Total cells/field (mean ± SE)	Average % viability	% cells transduced (mean ± SE)	Significantly different from no paclitaxel?
SCC-9	0	806 ± 55	100	31.0 ± 0.8	
	1	772 ± 56	96	39.0 ± 1.4	Yes ($P \leq 0.004$)
	2.5	738 ± 51	92	89.4 ± 1.4	Yes ($P \leq 0.003$)
	5	820 ± 84	102	42.8 ± 2.6	Yes ($P \leq 0.006$)
	7.5	823 ± 78	102	45.2 ± 0.8	Yes ($P \leq 0.0001$)
	10	749 ± 41	93	50.0 ± 4.4	Yes ($P \leq 0.007$)
SCC-15	0	1247 ± 91	100	21.4 ± 0.8	
	1	1175 ± 94	94	27.2 ± 2.7	No ($P \leq 0.06$)
	2.5	1028 ± 12	82	32.1 ± 0.7	Yes ($P \leq 0.0002$)
	5	1102 ± 59	88	31.9 ± 0.9	Yes ($P \leq 0.0004$)
	7.5	1045 ± 85	84	32.7 ± 2.1	Yes ($P \leq 0.0035$)
	10	995 ± 37	80	33.9 ± 0.7	Yes ($P \leq 0.0002$)
SCC-25	0	567 ± 26	100	30.9 ± 1.5	
	1	556 ± 27	98	38.0 ± 1.6	Yes ($P \leq 0.02$)
	2	533 ± 9	94	51.1 ± 1.0	Yes ($P \leq 0.0002$)
	2.5	523 ± 11	92	52.0 ± 0.8	Yes ($P \leq 0.0002$)
	5	528 ± 8	93	52.8 ± 2.0	Yes ($P \leq 0.0005$)
	10	516 ± 24	91	64.4 ± 0.8	Yes ($P \leq 0.0001$)
SK-OV-3	0	784 ± 30	100	11.6 ± 1.4	
	0.0001	721 ± 14	92	18.1 ± 1.5	Yes ($P \leq 0.02$)
	0.001	661 ± 25	84	26.7 ± 1.0	Yes ($P \leq 0.0005$)
	0.01	540 ± 5	69	35.5 ± 3.9	Yes ($P \leq 0.002$)
	0.1	369 ± 21	47	40.7 ± 2.8	Yes ($P \leq 0.0001$)
	1.0	333 ± 3	42	47.1 ± 1.4	Yes ($P \leq 0.0003$)
OVCAR-3	0	1140 ± 28	100	41.4 ± 3.5	
	1	1110 ± 74	97	52.3 ± 1.4	Yes ($P \leq 0.02$)
	2.5	1035 ± 27	91	55.7 ± 3.4	Yes ($P \leq 0.02$)
	5	920 ± 94	81	61.5 ± 3.1	Yes ($P \leq 0.007$)
	7.5	1033 ± 38	91	57.7 ± 1.6	Yes ($P \leq 0.007$)
	10	829 ± 74	73	65.4 ± 1.7	Yes ($P \leq 0.002$)
DU-145	0	934 ± 59	100	6.4 ± 0.2	
	2	917 ± 77	98	9.6 ± 0.6	Yes ($P \leq 0.003$)
	5	738 ± 47	79	20.5 ± 1.4	Yes ($P \leq 0.0002$)
	10	540 ± 84	58	34.9 ± 2.01	Yes ($P \leq 0.0001$)
	12.5	702 ± 32	75	41.1 ± 1.2	Yes ($P \leq 0.0001$)
MB-231	0	478 ± 10	100	46.8 ± 1.0	
	1	410 ± 34	86	57.7 ± 2.4	Yes ($P \leq 0.006$)
	5	358 ± 10	75	70.2 ± 3.7	Yes ($P \leq 0.022$)
	10	374 ± 24	78	69.4 ± 2.1	Yes ($P \leq 0.0003$)
MB-468	0	959 ± 78	100	4.9 ± 0.8	
	1	972 ± 48	101	9.0 ± 1.4	Yes ($P \leq 0.03$)
	2.5	941 ± 71	98	26.9 ± 2.7	Yes ($P \leq 0.0007$)
	5	672 ± 30	70	40.8 ± 4.8	Yes ($P \leq 0.0009$)
	7.5	699 ± 26	67	37.6 ± 4.6	Yes ($P \leq 0.001$)
	10	663 ± 20	69	38.2 ± 1.1	Yes ($P \leq 0.0001$)

weighed on day 27. Final tumor burden in mice treated only with drug vehicles was 1.01 ±0.14 g ($n = 10$). Treatment with p53 Ad reduced tumor burden 33% to 0.67 ± 0.05 g ($n = 10$). Treatment with paclitaxel reduced tumor burden 70% to 0.30 ± 0.02 g g ($n = 10$). When both drugs were combined, there was a further 90% reduction in tumor burden compared to paclitaxel alone to 0.03 ± 0.02 g ($n = 9$; $P \leq 0.0001$).

Efficacy in the DU-145 Prostate Tumor Model *in Vivo*. The efficacy of p53 Ad in combination with paclitaxel was also evaluated in the DU-145 xenograft model. As shown in Fig. 7, the combination of p53 Ad and paclitaxel reduced tumor burden 54% more than paclitaxel treatment by itself ($n = 10$ mice per group; $P \leq 0.0002$).

Efficacy in the MDA-MB-468 Mammary Tumor Model *in Vivo*. Established s.c. MDA-MB-468 tumors were treated with vehicles, p53 Ad, paclitaxel, or both drugs on days 0–4 and 7–10. As shown in Fig. 8, p53 Ad had greater efficacy when it was administered in combination with paclitaxel (days 7–21, $P \leq 0.0004$).

Efficacy in the MDA-MB-231 Mammary Tumor Model *in Vivo*. Established MDA-MB-231 breast carcinomas were treated with vehicles, paclitaxel, p53 Ad, or both drugs on days 0–4 and 8–11. As shown in Fig. 9, p53 Ad had enhanced efficacy when it was combined with paclitaxel (days 8–24, $P \leq 0.0003$).

Discussion

Synergy (or antagonism) between two chemical agents is an *in vitro* empirical phenomenon, in which the observed effect of the combination is more (or less) than what would be predicted from the effects of each agent working alone. Although *in vitro* synergy is not directly provable in the clinical setting, it

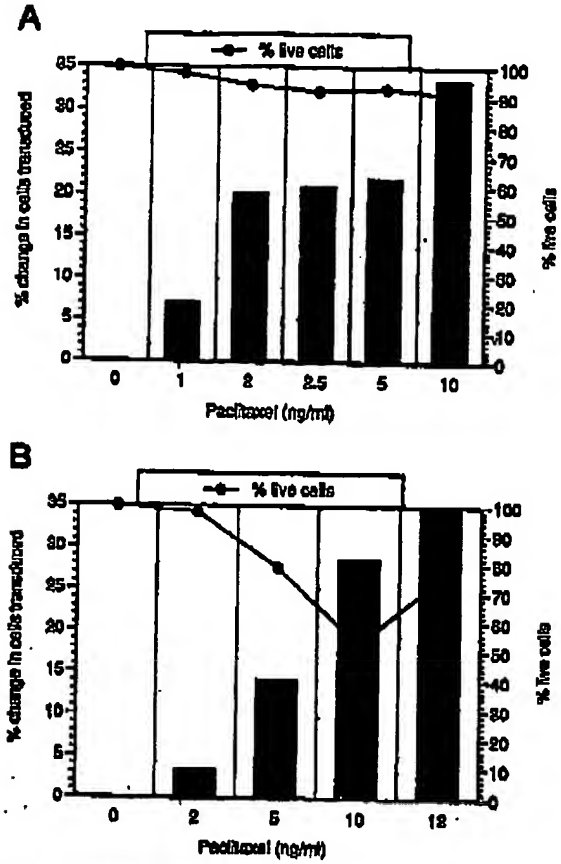

Fig. 4 Paclitaxel increased the percentage of cells transduced by β-gal Ad, independent of antiproliferative efficacy. *A*, SCC-25 cells; *B*, DU-145 cells.

does predict a favorable outcome when the two therapeutics are combined. In contrast, overt antagonism warns of future problems. Sophisticated statistical modeling techniques were used to evaluate the presence of synergistic, additive, or antagonistic efficacy between p53 Ad and paclitaxel (Taxol) in a panel of human tumor cell lines with nonfunctional p53. Tumor cells were treated with paclitaxel 24 h before p53 Ad or treated with both agents simultaneously. Paclitaxel had synergistic or additive efficacy in combination with p53 Ad, independent of whether the cells expressed mutant p53 protein or no p53 protein at all. Most importantly, antagonism between the two drugs was never observed.

p53 Ad arrested cells in G_0/G_1 prior to apoptotic cell death, consistent with the known activity of wild-type p53 in cells with damaged DNA (2). Paclitaxel arrested cells in G_2-M prior to apoptotic cell death, also consistent with previously published reports (8, 9). When the two drugs were combined in MDA-MB-231 cells, the relative concentration of each agent determined the dominant cellular response. These results are consistent with the cell cycle observations of Wahl *et al.* (9), which suggested that p53 facilitates progression through mitosis in cells exposed to paclitaxel and that cells with functional p53 accumulate in G_0/G_1 following completion of mitosis after paclitaxel exposure. However, published cell cycle data fail to explain the synergy observed between p53 Ad and paclitaxel in our experiments. Debernardis *et al.* (30) reported that the p53 status of a panel of ovarian tumor cells did not correlate with their sensitivity to paclitaxel-induced cell death. This report lends support to the view that the synergy observed between p53 Ad and paclitaxel may be due, at least in part, to an interaction between the Ad vector and paclitaxel. However, the fact that p53 can be coprecipitated with β-tubulin leaves open the possibility of interactions between p53 and downstream effectors of paclitaxel activity (31). In $p53^{wt}$ LNCaP prostate tumor cells, paclitaxel down-regulates expression of bcl-x_L, a member of the *bcl-2* gene family, which protects cells from apoptosis (32). p53 has been shown to down-regulate expression of the antiapoptotic *bcl-2* gene and up-regulate expression of the pro-apoptotic *bax* gene in other tumor cells (1–3). Therefore, p53 and paclitaxel may potentiate each other in stimulating the apoptotic pathway in neoplastic cells.

Our results suggest that paclitaxel increases cell transduction by recombinant Ad in a dose-dependent manner. Although it is possible to consider a scenario in which cells containing only one or a few Ads do not express detectable β-gal enzyme activity until hyperstimulation by paclitaxel, this scenario is highly unlikely. Transgene expression in this Ad vector is driven by the strong cytomegalovirus promoter on a continuous basis in cells, starting shortly after infection by recombinant Ad. Also, the signal from every enzyme molecule is amplified in the detection assay. The most likely interpretation of our results is that paclitaxel increases the number of cell infected by Ad. This is one possible mechanism to explain the observation of drug synergy. In other words, we hypothesize that more tumor cells are infected with p53 Ad and exposed to high levels of wild-type p53 protein when paclitaxel "sensitizes" them to transduction by recombinant Ad. Of particular note, the concentrations of paclitaxel responsible for increased Ad transduction are lower than the concentrations required for microtubule condensation. Also, the rate of change in the number of cells transduced by Ad appears to be independent of paclitaxel-induced cell death. The paclitaxel literature offers few clues as to possible mechanisms for the Ad transduction effect. Paclitaxel concentrations below 10 nM inhibit microtubule organization and mitosis in HeLa cells without increasing the mass of microtubule polymers (33). The alteration of mitotic spindle organization is similar to that induced by *Vinca* alkaloids, such as vinblastine. At 100 nM, paclitaxel suppresses both addition and loss of bovine brain tubulin monomers at the ends of microtubules, resulting in stabilization of microtubule lengths (33). At 10 nM, paclitaxel suppresses the shortening rate with no effect on the growth rate (34). Little is known about the process of cell transduction by Ad and specifically, the role of microtubules in the process. It is possible that stabilized microtubules assist virus transport within cells more readily than do normal, dynamic microtubules.

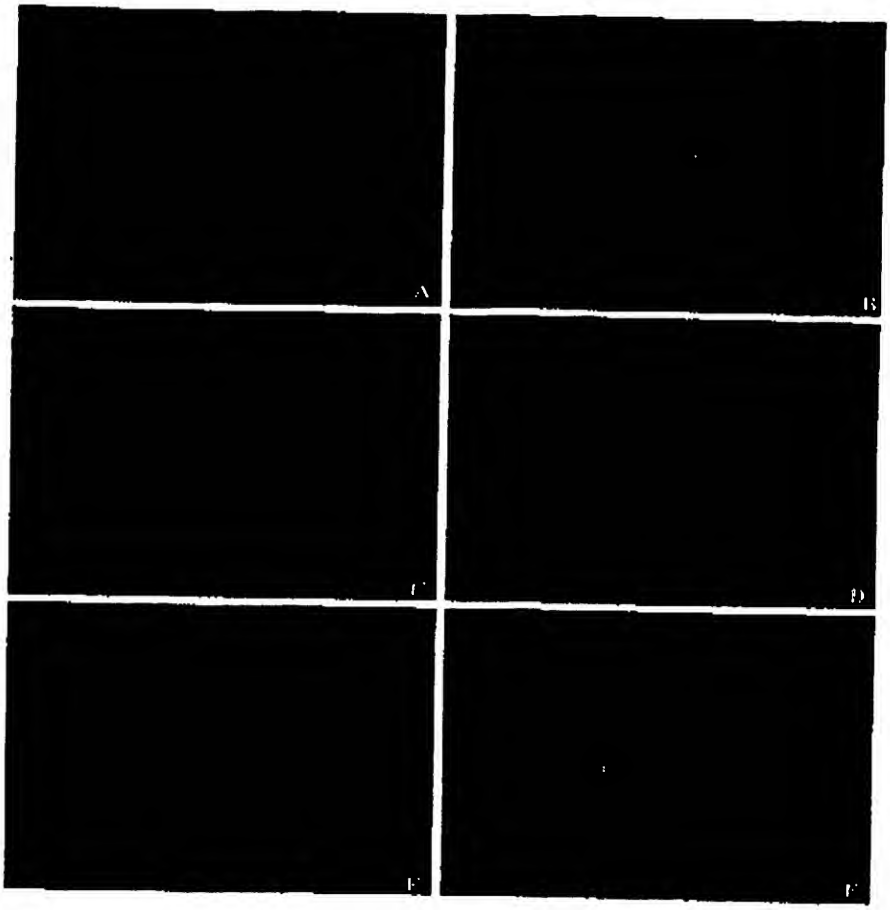

Fig. 5 Immunofluorescent microtubules in MDA-MB-231 cells, untreated (*A*) or treated with 12 nM (10 ng/ml) paclitaxel (*C*) or 50 μM (43 μg/ml) paclitaxel (*B* and *D*), and in DU-145 cells, treated with 12 nM (10 ng/ml) paclitaxel (*E*) or 50 μM (43 μg/ml) paclitaxel (*F*). Note the increased microtubule branching at 12 nM paclitaxel and extensive microtubule condensation at 50 μM paclitaxel.

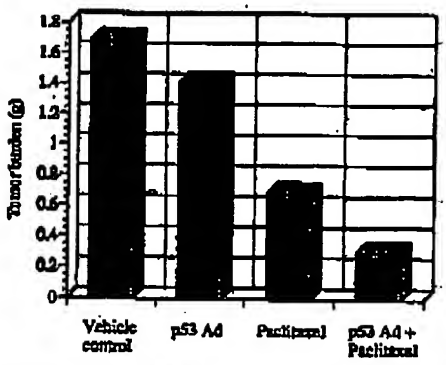

Fig. 6 Greater combined efficacy of p53 Ad and paclitaxel against SK-OV-3 ovarian xenografts in scid mice. *Columns*, means; *bars*, SE.

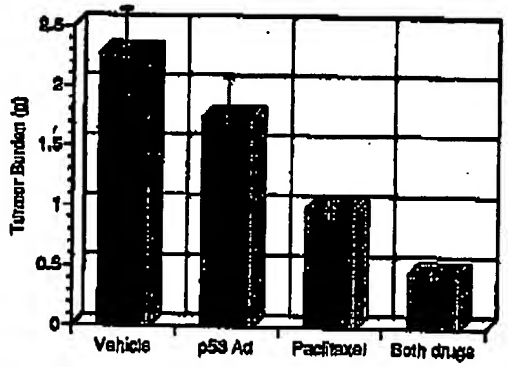

Fig. 7 Greater combined efficacy of p53 Ad and paclitaxel against DU-145 prostate xenografts in scid mice. *Columns*, means; *bars*, SE.

Christen *et al.* (31) reported that paclitaxel concentrations up to 900 nM had no effect on trypan blue exclusion from 2008 ovarian carcinoma cells, indicating that paclitaxel did not cause a generalized permeabilization of the plasma membrane. However, cisplatin accumulation increased approximately 50% over the same paclitaxel concentration range through a mechanism which appears to be related to microtubule stabilization by paclitaxel. In other experiments,

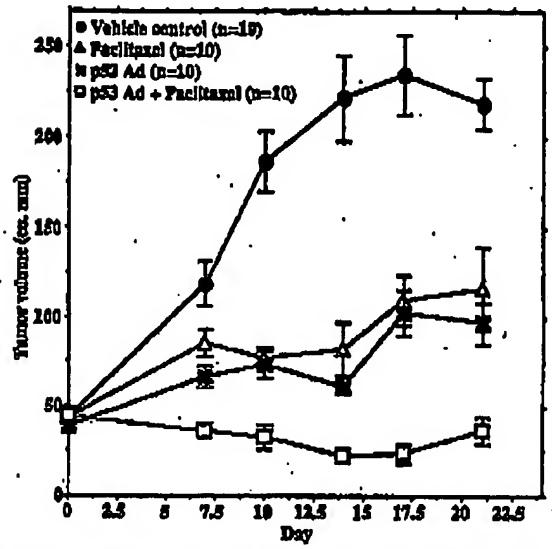

Fig. 8 Greater combined efficacy of p53 Ad and paclitaxel against MDA-MB-468 breast carcinoma xenografts in scid mice. *Data points*, means; *bars*, SE.

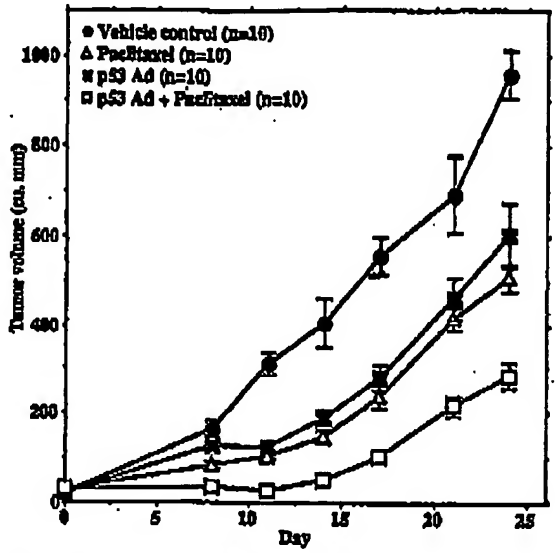

Fig. 9 Greater combined efficacy of p53 Ad and paclitaxel against MDA-MB-231 breast carcinoma xenografts in scid mice. *Data points*, means; *bars*, SE.

irradiation increased the number of NIH-3T3 human fibroblast, 39F human fibroblast, and A549 human lung carcinoma cells transduced by a recombinant Ad expressing β-gal (35). However, as with paclitaxel, the mechanism is currently unknown.

The antitumor effects of combination therapy with p53 Ad and paclitaxel were also evaluated *in vivo*. It has been well documented that p53 Ad is a drug with antitumor efficacy attributable to both the *p53* tumor suppressor gene and the Ad delivery vector (5). The *in vivo* experiments were designed to mimic the clinical situation in which efficacy of the p53 Ad drug (with or without chemotherapy) will be compared to clinical outcome with traditional chemotherapy. In this situation, it is unethical and prohibitively expensive to include study arms for an empty Ad vector. In a model of ovarian cancer, a dose of p53 Ad that had relatively minimal antitumor effect by itself had significantly enhanced efficacy when combined with paclitaxel. Paclitaxel also enhanced the antitumor efficacy of p53 Ad in models of human prostate and breast cancer. Taken together, our preclinical data support the evaluation of this combination in clinical trials. These data offer the possibility of enhanced antitumor activity with lower-than-normal doses of paclitaxel and p53 Ad, when the two drugs are administered in combination. This could potentially decrease chemotherapy-induced side effects, increasing patient quality of life and, perhaps, reducing the overall expense of a complete course of cancer therapy.

Investigations into the efficacy of *p53* gene therapy in combination with DNA-damaging agents have started appearing in the scientific literature over the last few years. However, none of these studies used rigorous methods to evaluate the type of drug interaction, if any, between *p53* gene therapy and DNA-damaging agents. Fujiwara *et al.* (36) demonstrated an additive antiproliferative effect in $p53^{null}$ H358 lung cancer when *p53* gene therapy was combined with cisplatin. H358 cells cultured with cisplatin for 24 h before transduction with p53 Ad had a significantly lower rate of proliferation than cells treated with either agent alone. When cells were transduced with p53 Ad 24 h before exposure to cisplatin, there was a dose-dependent cisplatin effect. H358 cells or H358 spheroids exposed to both agents exhibited greater apoptosis, as evidenced by DNA fragmentation. Enhanced efficacy when both agents were combined was also demonstrated *in vivo*. However, their *in vivo* studies were somewhat flawed in that they exceeded the maximum tolerated dose for cisplatin in mice in one experiment. More convincing *in vivo* evidence came from Nguyen *et al.* (37). In this study, $p53^{null}$ H1299 lung tumor xenografts were dosed with i.p. cisplatin before, concurrent with, or after intratumoral p53 Ad. The most effective dosing regime was cisplatin given two days before three doses of p53 Ad, with the Ad doses administered 2 days apart. A second cycle of therapy produced increased efficacy over a single cycle.

Qjerset *et al.* (38) demonstrated increased sensitivity to cisplatin cytotoxicity in $p53^{mut}$ T98G glioblastoma and $p53^{mut}$ H23 small cell lung carcinoma cells transduced with p53 expression vectors 1 or 2 days before cisplatin exposure. Cell death mediated by apoptosis was significantly increased when T98G cells were transduced by p53 Ad 2 days before exposure to cisplatin, as compared to cells only exposed to p53. Enhanced efficacy was also seen for the combination of p53 and γ-irradiation. Yang *et al.* (39) used $p53^{mut}$ SW480 colorectal tumor cells transfected with an isopropyl-1-thio-β-D-galactopyranoside-inducible p53 plasmid construct to

evaluate the combined efficacies of p53 with 5-FU, topotecan, or γ-irradiation. All three agents displayed dose-dependent effects on cell cytotoxicity that were enhanced by concurrent expression of wild-type p53. DNA fragmentation was elevated in cells exposed to both p53 and 5-FU. Further, the potentiation of 5-FU cytotoxicity by p53 was greatest when cells were exposed to both agents simultaneously. Blagosklonny and El-Deiry (40) reported increased cell killing in $p53^{mut}$ SkBr3 mammary tumor cells when transduction with p53 Ad was followed 8 h later by doxorubicin or mitomycin C but not by vincristine. Greater combined efficacy was not observed in $p53^{wt}$ MCF-7 mammary tumor cells for any of these three chemotherapy drugs.

Additional studies on the ability of wild-type p53 to sensitize tumor cells to irradiation have been reported for colorectal and ovarian tumor cells (41, 42). SW620 colorectal tumor cells ($p53^{mut}$) were transduced with p53 Ad 48 h before irradiation (41). Cell survival was reduced by 50–66% compared to mock- or vector-infected irradiated cells, and this reduction was mediated by apoptotic cell death. Efficacy was also highest in SW620 xenografts pretreated with three consecutive doses of p53 Ad before irradiation. Again, apoptosis was most evident in tumors treated with both agents. Similar, although not as dramatic, results have been reported for $p53^{null}$ SK-OV-3 ovarian tumor cells (42). Cells transduced with p53 Ad and subsequently irradiated had lower survival than mock- or vector-infected irradiated cells. s.c. tumor xenografts were treated once with p53 Ad or the appropriate controls and then irradiated on 3 consecutive days. This dosing regime was repeated 1 week later. Combination therapy with p53 and irradiation had significantly increased efficacy against tumor xenografts and cured 45% of the mice.

The conclusion from published studies is that *p53* gene therapy combined with DNA-damaging agents has additional efficacy over p53 gene therapy alone. In particular, cisplatin pretreatment might sensitize tumors to subsequent p53 gene therapy. There are no previous reports on the combination of p53 gene therapy with paclitaxel, which acts by the much different mechanism of altering microtubule dynamics within cells.

Acknowledgments

We thank Drs. Bill Demers, Dan Maneval, and Lydia Armstrong for helpful discussions.

References

1. Ozbun, M. A., and Butel, J. S. Tumor suppressor *p53* mutations and breast cancer: a critical analysis. Adv. Cancer Res., *66:* 71–141, 1995.

2. Selter, H., and Montenarh, M. The emerging picture of p53. Int. J. Biochem., *26:* 145–154, 1994.

3. Thompson, C. B. Apoptosis in the pathogenesis and treatment of disease. Science (Washington DC), *267:* 1456–1462, 1995.

4. Donehower, L. A., Harvey, M., Slagle, B. L., McArthur, M. J., Montgomery, C. A., Butel, J. S., and Bradley, A. Mice deficient for p53 are developmentally normal but susceptible to spontaneous tumours. Nature (Lond.), *356:* 215–221, 1992.

5. Nielsen, L. L., and Maneval, D. p53 tumor suppressor gene therapy for cancer. Cancer Gene Ther., *5:* 52–63, 1998.

6. Horwitz, S. B. Mechanism of action of Taxol. Trends Pharmacol. Sci., *13:* 134–136, 1992.

7. Rowinsky, E. K., Cazenave, L. A., and Donehower, R. C. Taxol: a novel investigational antimicrotubule agent. J. Natl. Cancer Inst. (Bethesda), *82:* 1247–1259, 1990.

8. Donaldson, K. L., Goolsby, G. L., and Wahl, A. F. Cytotoxicity of the anticancer agents cisplatin and Taxol during cell proliferation and the cell cycle. Int. J. Cancer, *57:* 847–855, 1994.

9. Wahl, A. F., Donaldson, K. L., Fairchild, C., Lee, F. Y. F., Foster, S. A., Demers, G. W., and Galloway, D. A. Loss of normal p53 function confers sensitization to Taxol by increasing G_2-M arrest and apoptosis. Nat. Med., *2:* 72–79, 1996.

10. Berenbaum, M. C. What is synergy? Pharmacol. Rev., *41:* 93–141, 1989.

11. Wills, K. N., Maneval, D. C., Menzel, P., Harris, M. P., Sutjipto, S., Vaillancourt, M-T., Huang, W-M, Johnson, D. E., Anderson, S. C., Wen, S. F., Bookstein, R., Shepard, H. M., and Gregory, R. J. Development and characterization of recombinant adenoviruses encoding human p53 for gene therapy of cancer. Hum. Gene Ther., *5:* 1079–1088, 1994.

12. Harris, M. P., Sutjipto, S., Wills, K. N., Hancock, W., Connell, D., Johnson, D. E., Gregory, R. J., Shepard, H. M., and Maneval, D. C. Adenovirus-mediated p53 gene transfer inhibits growth of human tumor cells expressing mutant p53 protein. Cancer Gene Ther., *3:* 121–130, 1996.

13. Nielsen, L. L., Dell, J., Maxwell, E., Armstrong, L, Maneval, D., and Catino, J. J. Efficacy of p53 adenovirus-mediated gene therapy against human breast cancer xenografts. Cancer Gene Ther., *4:* 129–138, 1997.

14. Bartek, J., Iggo, R., Gannon, J., and Lane, D. P. Genetic and immunochemical analysis of mutant p53 in human breast cancer cell lines. Oncogene, *5:* 893–899, 1990.

15. Isaacs, W. B., Carter, B. S., and Ewing, C. M. Wild-type *p53* suppresses growth of human prostate cancer cells containing mutant *p53* alleles. Cancer Res., *51:* 4716–4720, 1991.

16. Yagihama, Y., and Westphal, H. Abnormal structure and expression of the *p53* gene in human ovarian carcinoma cell lines. Cancer Res., *52:* 4196–4199, 1992.

17. Jung, M., Notario, V., and Dritschilo, A. Mutations in the p53 gene in radiation-sensitive and -resistant human squamous carcinoma cells. Cancer Res., *52:* 6390–6393, 1992.

18. Cummo, J., Zhang, S. Y., Rosvold, E. A., Bauer, B., and Klein-Szanto, A. J. P. p53 alterations in human squamous cell carcinomas and carcinoma cell lines. Am. J. Pathol., *142:* 1131–1139, 1993.

19. Min, B., Baek, J., Shin, K., Gujuluva, C. N., Chertick, H. M., and Park, N. Inactivation of the p53 gene by either mutation or HPV infection is extremely frequent in human oral squamous cell carcinoma cell lines. Eur. J. Cancer, *30B:* 338–345, 1994.

20. Huyghe, B. G., Liu, X., Sutjipto, S., Sugarman, B. J., Horn, M. T., Shepard, H. M., Scandella, C. J., and Shabram, P. Purification of a type 5 recombinant adenovirus encoding human p53 by column chromatography. Hum. Gene Ther., *6:* 1403–1416, 1995.

21. Mosmann, T. Rapid colorimetric assay for cellular growth and survival: application to proliferation and cytotoxicity assays. J. Immunol. Methods, *64:* 55–63, 1983.

22. Greco, W. R., Bravo, G., and Parsons, J. C. The search for synergy: a critical review from a response surface perspective. Pharmacol. Rev., *47:* 331–385, 1995.

23. Hardy, R. L., and Desmarais, R. N. Interpolation using surface splines. J. Aircraft, *9:* 189–191, 1972.

24. SAS Institute Inc. SAS/GRAPH Software: Reference, Version 6, Ed. 1, Vol. 2. Cary, NC: SAS Institute Inc., 1990.

25. Snyder, W. V. Contour plotting [J6]. ACM Trans. Math. Software, *4:* 290–294, 1978.

26. Berenbaum, M. C. Criteria for analyzing interactions between biological active agents. Adv. Cancer Res., *35:* 269–333, 1981.

27. Carter, W. H., Gennings, C., Staniswalis, J. G., Campbell, E. D., and White, K. L. A statistical approach to the construction and analysis of isobolograms. J. Am. Coll. Toxicol., *7:* 963–973, 1988.

28. SAS Institute Inc. SAS/STAT Software. Changes and Enhancements through Release 6.12. Cary, NC: SAS Institute Inc., 1997.

29. O'Connell, and Wolfinger, R. D. Spatial regression models, response surfaces, and process optimization. J. Comput. Graph. Stat., *6:* 224–241, 1997.

30. Debernardis, D., Sire, B. G., De Feudis, P., Vikhanskaya, F., Valenti, M., Russo, P., Parodi, S., D'Incalci, M., and Broggini, M. p53 status does not affect sensitivity of human ovarian cancer cell lines to paclitaxel. Cancer Res., *57:* 870–874, 1997.

31. Christen, R. D., Jekunen, A. P., Jones, J. A., Thiebaut, F., Shalinsky, D. R., and Howell, S. B. *In vitro* modulation of cisplatin accumulation in human ovarian carcinoma cells by pharmacologic alteration of microtubules. J. Clin. Invest., *92:* 431–440, 1993.

32. Liu, Q., and Stein, C. A. Taxol and estramustine-induced modulation of human prostate cancer cell apoptosis via alteration in bcl-x_L and bak expression. Clin. Cancer Res., *3:* 2039–2046, 1997.

33. Jordan, M. A., Toso, R. J., Thrower, D., and Wilson, L. Mechanism of mitotic block and inhibition of cell proliferation by Taxol at low concentrations. Proc. Natl. Acad. Sci. USA, *90:* 9552–9556, 1993.

34. Derry, W. B., Wilson, L., and Jordan, M. A. Substoichiometric binding of Taxol suppresses microtubule dynamics. Biochemistry, *34:* 2203–2211, 1995.

35. Zheng, M., Cerniglia, G. J., Eck, S. L., and Stevens, C. W. High-efficiency stable gene transfer of adenovirus into mammalian cells using ionizing radiation. Hum. Gene Ther., *8:* 1025–1032, 1997.

36. Fujiwara, T., Grimm, E. A., Mukhopadhyay, T., Zhang, W-W., Owen-Schaub, L. B., and Roth, J. A. Induction of chemosensitivity in human lung cancer cells *in vivo* by adenovirus-mediated transfer of the wild-type *p53* gene. Cancer Res., *54:* 2287–2291, 1994.

37. Nguyen, D. M., Spitz, F. R., Yen, N., Cristiano, R. J., and Roth, J. A. Gene therapy for lung cancer: enhancement of tumor suppression by a combination of sequential systemic cisplatin and adenovirus-mediated p53 gene transfer. J. Thorac. Cardiovasc. Surg., *112:* 1372–1377, 1996.

38. Gjerset, R. A., Turla, S. T., Sobol, R. E., Scalise, J. J., Mercola, D., Collins, H., and Hopkins, P. J. Use of wild-type p53 to achieve complete treatment sensitization of tumor cells expressing endogenous mutant p53. Mol. Carcinog., *14:* 275–285, 1995.

39. Yang, B., Eshleman, J. R., Berger, N. A., and Markowitz, S. D. Wild-type p53 protein potentiates cytotoxicity of therapeutic agents in human colon cancer cells. Clin. Cancer Res., *2:* 1649–1657, 1996.

40. Blagosklonny, M., and El-Deiry, W. S. *In vitro* evaluation of a p53-expressing adenovirus as an anti-cancer drug. Int. J. Cancer, *67:* 386–392, 1996.

41. Spitz, F. R., Nguyen, D., Skibber, J. M., Meyn, R. E., Cristiano, R. J., and Roth, J. A. Adenoviral-mediated wild-type *p53* gene expression sensitizes colorectal cancer cells to ionizing radiation. Clin. Cancer Res., *2:* 1665–1671, 1996.

42. Gallardo, D., Drazan, K. E., and McBride, W. H. Adenovirus-based transfer of wild-type p53 gene increases ovarian tumor radiosensitivity. Cancer Res., *56:* 4891–4893, 1996.